

# Dynamic Magnetization Model of Nonoriented Steel Sheets

Simon Steentjes<sup>1</sup>, Sergey E. Zirka<sup>2</sup>, Yuriy E. Moroz<sup>2</sup>, Elena Y. Moroz<sup>2</sup>, and Kay Hameyer<sup>1</sup>

<sup>1</sup>Institute of Electrical Machines, RWTH Aachen University, Aachen 52056, Germany

<sup>2</sup>Dnepropetrovsk National University, Dnepropetrovsk 49050, Ukraine

**A simplified model of conducting ferromagnetic sheet, which describes magnetization of isotropic electrical steels is proposed. The model improvement is achieved by determining eddy current component of the magnetic field at the sheet surface in the framework of the method by Wolman and Kaden, which describes the dynamic magnetization of the material with rectangular hysteresis loop. An algorithm of model fitting is proposed and a comparison of calculated and experimental results has been carried out.**

**Index Terms**—Dynamic magnetization model, eddy currents, electrical steels, excess losses, magnetic hysteresis, saturation wave model (SWM).

## I. INTRODUCTION

**T**HE reliable description of transformers, rotating electrical machines, and other devices containing ferromagnetic cores requires considering magnetic hysteresis, induced eddy currents and so-called excess (anomalous) loss, which is caused by the domain structure of ferromagnetic materials [1]. In the widespread case, when the shortest and longest magnetic flux paths in the core are not too different, the analysis of its magnetization is reduced to the modeling of the transient behavior in a single sheet [2]. The ideal solution of such a problem would be a model, which allows predicting both the specific loss and the shape of hysteresis loop at arbitrary magnetization regimes.

A sufficiently accurate description of transients in the laminated nonoriented (NO) steel can be obtained using a magnetodynamic model (MDM) [2], which is a finite-difference (FD) solver of the classical Maxwell (penetration or diffusion) equation

$$\rho \frac{\partial^2 \mathbf{H}}{\partial x^2} = \frac{\partial \mathbf{B}}{\partial t} \quad (1)$$

where vectors of the magnetic field strength  $\mathbf{H}(x, t)$  and magnetic flux density  $\mathbf{B}(x, t)$  are directed along the sheet; axis  $x$  is normal to its surface, and  $\rho$  is the electrical resistivity of the steel. When solving (1) numerically, magnetic flux density  $B_k(t)$  and field  $H_k(t)$  in a node  $k$  of the computational grid are linked by a static hysteresis dependence  $H_h(B)$ , in which the unaccounted (excess) loss is reproduced by implementing a time delay of  $B_k(t)$  behind  $H_k(t)$ .

As shown in [2], the solution of the partial derivative (1) can be reduced to the integration of  $N$  simultaneous ordinary differential equations for  $B_k(t)$  and  $H_k(t)$ . To gain sufficient accuracy, the number of nodes  $N$  of the FD grid should reach 15–25, and for each of the nodes the history of the magnetization process should be tracked and updated if a history-dependent hysteresis model is employed. When analyzing devices with branched magnetic topology, the dimension of the problem increases proportionally to the number of branches leading to a quite complicated and time-consuming model.

Substantial simplification of the problem, while keeping sufficiently accurate solution, can be achieved by a thin sheet model (TSM), which links the magnetic field at the sheet surface  $H(t)$  and the mean magnetic flux density  $B(t)$  over its cross section [1], [3], [4]. The magnetic field  $H(t)$  in such a model is represented by the sum of hysteresis, induced eddy current (classical) and excess components,  $H(t) = H_h + H_{\text{clas}} + H_{\text{exc}}$ . For example, the TSM in [3], [4] is written by

$$H(t) = H_h(t) + \frac{d^2}{12\rho} \frac{dB}{dt} + g(B)\delta \left| \frac{dB}{dt} \right|^{1/\alpha} \quad (2)$$

where  $d$  is the sheet thickness and  $\delta = \text{sign}(dB/dt)$ . Among the advantages of (2) relative to other TSMs is its possibility to change frequency properties of the model (by choosing  $\alpha$ ) and to control the shape of dynamic hysteresis loops by choosing function  $g(B)$ . Model (2) has shown considerable accuracy being applied to grain oriented [4] and some NO steels with sheet thickness 0.1 mm and high silicon content (5.5 and 6.5 wt%) [3]. Simultaneously, this model is less accurate in describing high-frequency regimes of conventional NO steels, i.e., steels with the sheet thickness about 0.5 mm and silicon content not exceeding 3 wt%. The reason is the relatively low electrical resistivity of these steels and, thus, the error of the well-known formula for the so-called classical field [1]

$$H_{\text{clas}} = \frac{d^2}{12\rho} \frac{dB}{dt}. \quad (3)$$

However, the shortcoming of this approach lies in the fact, that the usual skin effect observed in a magnetically linear medium ( $\mu = \text{const}$ ) is absent here, leading to the wrong predictions of the eddy current field using the classical approach. For this reason, this paper proposes a TSM, improving the eddy current field description on the basis of physical ideas in the framework of the saturation wave model (SWM) [7].

To represent the layer-to-layer nature of the magnetization reversal, the classical eddy current component is replaced by the expression arising from the SWM. The hysteresis component is modeled using the static history-dependent hysteresis model (SHM) [10].

## II. IMPROVED TSM AND FITTING PROCEDURE

The solid curves in Fig. 1 show the static major loop of NO steel considered ( $B_p = 1.595$  T) and a minor symmetrical

Manuscript received August 2, 2013; revised September 22, 2013; accepted September 25, 2013. Date of current version April 4, 2014. Corresponding author: S. Steentjes (e-mail: simon.steentjes@iem.rwth-aachen.de).

Digital Object Identifier 10.1109/TMAG.2013.2284357

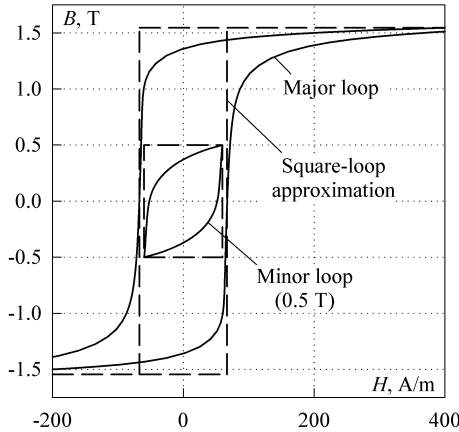
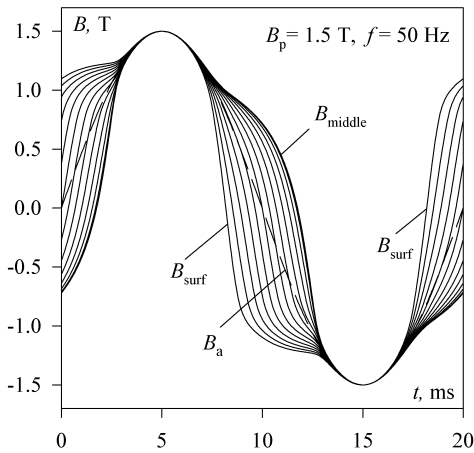
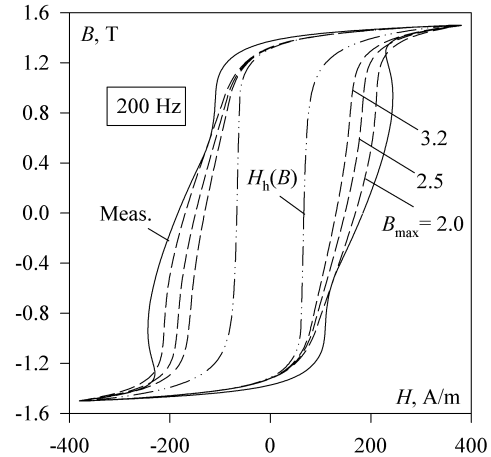


Fig. 1. Static loops of NO steel.

Fig. 2. Solid curves: flux densities at equidistant points from the surface to the middle of the sheet. Dashed curve: sinusoidal average magnetic flux density  $B_a$  versus time.

loop measured at  $B_p = 0.5$  T. It is obvious that their square-loop approximations (dashed lines in Fig. 1) are more accurate than any linear approximations of these loops (especially major loop). This suggests the idea that a better description of the magnetization dynamics of the steel can be carried out in the framework of the SWM originally proposed in [7] and then further developed in [8] and [9]. This model applies to a ferromagnetic material characterized by a step-like magnetization curve with maximum value  $B_{\max}$  and therefore can be applied to a material with a rectangular hysteresis loop (RHL) with the height  $2B_{\max}$ .

In accordance with the SWM, the magnetization reversal in the RHL material has a layer-to-layer nature and consists of successions of instant flux reversals in thin layers of the sheet (from  $-B_{\max}$  to  $+B_{\max}$  and back). The potential applicability of the SWM in the TSM is corroborated by the layer-wise flux reversal (Fig. 2) calculated using the MDM [2] at the sinusoidal average magnetic flux density  $B_a$  with an amplitude  $B_p = 1.5$  T and  $f = 50$  Hz. Similar to the process in the material with ideally square loop, maximum flux density in all layers of the sheet, including magnetic flux density  $B_{\text{surf}}$  at

Fig. 3. Sum of  $H_h(B)$  and  $H_{cc}(B, t)$  calculated for  $B_{\max} = 2.0, 2.5,$  and  $3.2$  T.

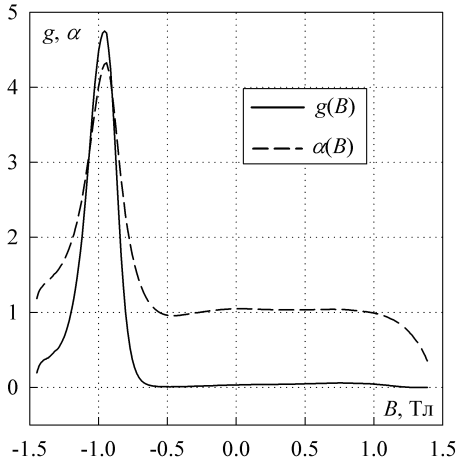
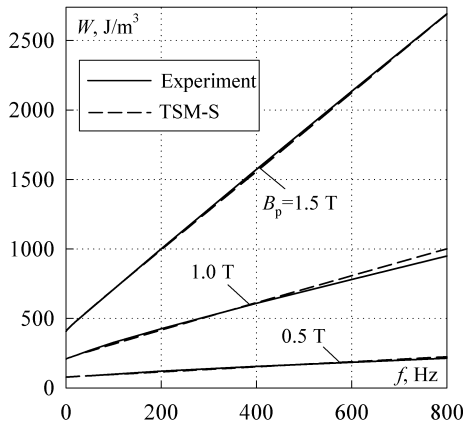
its surface and the magnetic flux density  $B_{\text{mid}}$  in the middle of the sheet, reaches the level of  $B_p = 1.5$  T, i.e., the usual skin effect observed in a magnetically linear medium is absent here. Therefore, the second term in (2) should be replaced by the expression arising from the SWM [7]

$$H_{cc}(B, t) = \frac{d^2(B - B_T) dB}{8\rho B_{\max} dt} \quad (4)$$

where  $B_T$  being the magnetic flux density in a turning point, which is the point, where derivative  $dB/dt$  changes its sign. Dashed curves in Fig. 3 show the sum of the hysteresis field  $H_h(B)$  and the induced eddy current field  $H_{cc}(B, t)$  calculated with (4) for several values of  $B_{\max}$  (2.0, 2.5, and 3.2 T). As these curves do not (or almost do not) go beyond the experimental loop, the field  $H_{\text{exc}}$  supplementing this sum to the measured field  $H(t)$ , is positive at any  $B(t)$ . Therefore, the proposed phenomenological model, referred to as TSM-S, is written as

$$H(t) = H_h(B) + \frac{d^2(B - B_T) dB}{8\rho B_{\max} dt} + g(B) \left| \frac{dB}{dt} \right|^{1/\alpha(B)}. \quad (5)$$

Since the static hysteresis loop of the real magnetic material is not perfectly square, the value of  $B_{\max}$  can be considered as a variable phenomenological parameter, which is chosen for a given material along with the functions  $\alpha(B)$  and  $g(B)$ . For a chosen value of  $B_{\max}$ , the required  $g(B)$  and  $\alpha(B)$  are configured so as the loops calculated for a fixed amplitude  $B_p$  were as close as possible to the loops measured at three to four frequencies (ensuring a stable and well-conditioned fitting process). Given the symmetry of the steady-state hysteresis loops, the model fitting can be made using  $n$  points of the ascending branches. For each such point (i.e., for a given level  $B_i$ ), a pair of  $\alpha_i$  and  $g_i$  are found so as to minimize the total deviation in  $H$  of calculated loops from the experimental ones for all chosen frequencies. The results from the above calculations are brought into the table containing  $\alpha_i(B_i)$  and  $g_i(B_i)$ , which can be approximated by splines  $\alpha(B)$  and  $g(B)$ . The calculations for the chosen  $B_{\max}$  are completed by building frequency dependencies of


 Fig. 4. Optimized functions  $g(B)$  and  $\alpha(B)$ .

 Fig. 5. Loss dependencies versus frequency measured and calculated at sinusoidal magnetic flux density with peak values  $B_p$ .

the specific iron losses for several values of  $B_p$  (the energy loss  $W$  per unit volume and cycle is calculated as the area of the corresponding dynamic loop). After comparing the calculated dependencies  $W(f)$  with experimental ones, the value of  $B_{\max}$  is corrected and the above procedure is repeated until a best fit of calculated and experimental curves  $W(f)$  is achieved.

### III. MODEL VERIFICATION

The parameter identification of the TSM-S (5) was carried out by three dynamic loops with  $B_p = 1.5$  T and  $f = 50, 200,$  and  $800$  Hz. The obtained dependencies  $\alpha(B)$  and  $g(B)$  are shown in Fig. 4. The best value of  $B_{\max}$  was found to be equal 2.9 T. Frequency dependencies of specific energy loss are shown in Fig. 5. The prediction of the loop shapes shown by the proximity of the measured and calculated dependencies  $W(f)$  in Fig. 5 is quite satisfactory in a wide range of frequency  $f$  and magnetic flux density (presented for three different levels of  $B_p$ ).

An indicator of the model quality is its ability to reproduce dynamic hysteresis loops at complex waveforms of the magnetization voltage. Figs. 6(a) and 7(a) compare the calculated and experimental loops corresponding to the pulswidth

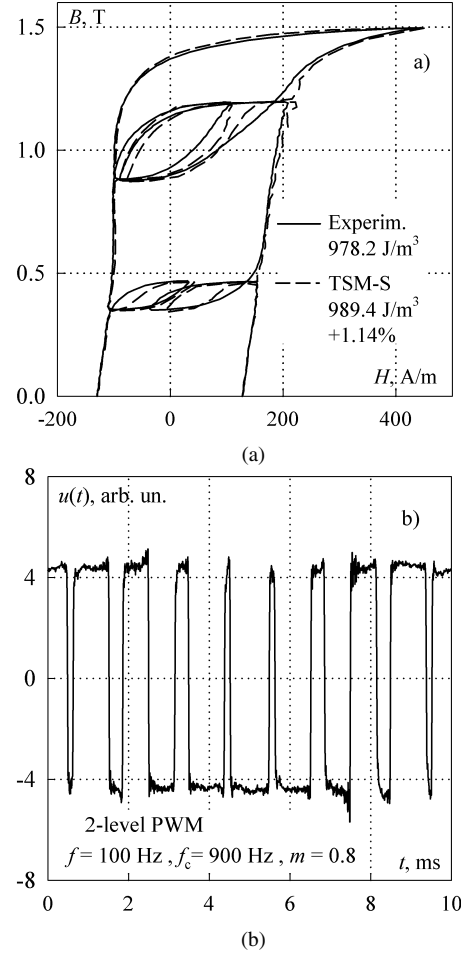


Fig. 6. (a) Dynamic loops calculated and measured at (b) two-level PWM.

modulation (PWM) voltages shown in Figs. 6(b) and 7(b). These are two-level voltage (PWM-2) and three-level voltage (PWM-3). Fundamental ( $f$ ) and carrier ( $f_c$ ) frequencies are 100 and 900 Hz, the modulation index  $m = 0.8$  [2].

The term  $H_h(B)$  in the implemented model (5) is found using the SHM [10], whose memory keeps the information about the history of the magnetization, i.e., about all turning points of unclosed minor loops and static curves  $H_h(B)$  connecting these points. When the minor loop is closed, the information about this loop is wiped out from the model memory, and the value of  $B_T$  in (5) is set equal to the  $B$ -coordinate of the initial point of the current curve stored in the memory of the SHM. Thus, at each turning point, the value of  $B_T$  gets a new value, which is kept until the next reversal occurs or the loop is closed. As shown in Figs. 6(a) and 7(a), the errors in the loss predictions for the voltages PWM-2 and PWM-3 are 1.1% and 2.0%, respectively.

Using the above examples of the PWM voltage, it is noted that if  $H(B)$  and  $B_T$  are calculated using a history-independent SHM (its simple version is also proposed in [2]), then the specific loss is underestimated by 24% (at PWM-2) and 16% (at PWM-3). Simultaneously, the

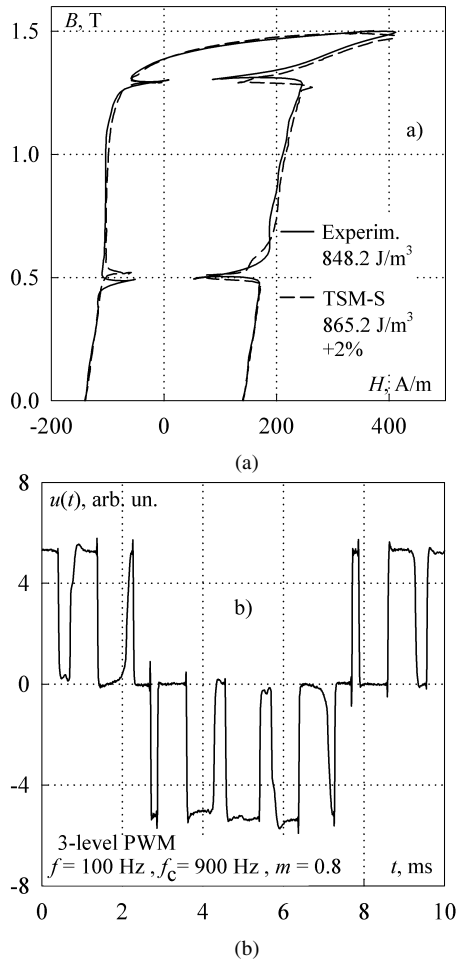


Fig. 7. (a) Dynamic loops calculated and (b) the three-level PWM voltage waveform.

simplest history-independent SHM can be used in the absence of minor loops superimposed on the major (outer) hysteresis loop.

#### IV. CONCLUSION

The motivation for this paper is the development of a time-efficient model of conducting ferromagnetic sheet, which describes magnetization of isotropic electrical steels considering magnetic hysteresis, induced eddy currents, and excess (anomalous) loss. Sufficiently accurate solutions can be obtained using a TSM. Improvement of the TSM proposed

is achieved by determining eddy current component of the magnetic field at the sheet surface in the framework of the method by Wolman and Kaden [7], which describes the dynamic magnetization of the material with an RHL. Thereby, the layer-to-layer nature of the magnetization process is considered.

The effectiveness of the proposed algorithm is confirmed by modeling a NO electrical steel with  $d = 0.5 \text{ mm}$  and  $\rho = 0.43 \cdot 10^{-6} \Omega\text{m}$  characterized in an Epstein frame with controlled sinusoidal magnetic flux density [2].

The model quality is also corroborated by its ability to reproduce dynamic hysteresis loops at complex waveforms of the magnetization voltage. This allows one to use the described model in analysis of transients in electrical circuits containing elements with ferromagnetic cores. This opens up the possibility of accurate evaluation of magnetic losses in real-life electrical engineering devices.

#### ACKNOWLEDGMENT

The work of Steentjes was granted by the Deutsche Forschungsgemeinschaft (DFG) carried out in the research project "Improved modelling and characterisation of ferromagnetic materials and their losses."

#### REFERENCES

- [1] G. Bertotti, *Hysteresis in Magnetism*. San Diego, CA, USA: Academic, 1998.
- [2] S. E. Zirka, Y. I. Moroz, P. Marketos, and A. J. Moses, "Viscosity-based magnetodynamic model of soft magnetic materials," *IEEE Trans. Magn.*, vol. 42, no. 9, pp. 2121–2132, Sep. 2006.
- [3] S. E. Zirka, Y. I. Moroz, P. Marketos, A. J. Moses, and D. C. Jiles, "Measurement and modeling of  $B$ - $H$  loops and losses of high silicon non-oriented steels," *IEEE Trans. Magn.*, vol. 42, no. 10, pp. 3177–3179, Oct. 2006.
- [4] S. E. Zirka, Y. I. Moroz, P. Marketos, A. J. Moses, D. C. Jiles, and T. Matsuo, "Generalization of the classical method for calculating dynamic hysteresis loops in grain-oriented electrical steels," *IEEE Trans. Magn.*, vol. 44, no. 9, pp. 2113–2126, Sep. 2008.
- [5] S. Steentjes, M. Leßmann, and K. Hameyer, "Semi-physical parameter identification for an iron-loss formula allowing loss-separation," *J. Appl. Phys.*, vol. 113, no. 17, pp. 17A319-1–17A319-3, 2013.
- [6] E. Dlala, "A simplified iron loss model for laminated magnetic cores," *IEEE Trans. Magn.*, vol. 44, no. 11, pp. 3169–3172, Nov. 2008.
- [7] W. Wolman and H. Kaden, "Über die Wirbelstromverzögerung magnetischer Schaltvorgänge," *Z. Tech. Phys.*, vol. 13, pp. 330–345, Jul. 1932.
- [8] M. A. Rozenblat, *Magnetic Elements of Automatic Devices and Computers*. Moscow, Russia: Nauka, 1974.
- [9] C. Serpico, C. Visone, I. D. Mayergoyz, V. Basso, and G. Miano, "Eddy current losses in ferromagnetic laminations," *J. Appl. Phys.*, vol. 87, no. 9, pp. 6923–6925, May 2000.
- [10] S. E. Zirka, Y. I. Moroz, P. Marketos, and A. J. Moses, "Congruency-based hysteresis models for transient simulations," *IEEE Trans. Magn.*, vol. 40, no. 2, pp. 390–399, Mar. 2004.